Atmos. Chem. Phys., 25, 12721–12735, 2025
https://doi.org/10.5194/acp-25-12721-2025
© Author(s) 2025. This work is distributed under
the Creative Commons Attribution 4.0 License.

Atmospheric Chemistry and Physics
Open Access
EGU

Hydroxymethanesulfonate (HMS) formation in urban and marine atmospheres: role of aerosol ionic strength

Rongshuang Xu[1,2], Yu-Chi Lin[1,2], Siyu Bian[1,2], Feng Xie[1,2], and Yan-Lin Zhang[1,2]

[1]School of Ecology and Applied Meteorology, Nanjing University of Information Science & Technology, Nanjing 210044, China
[2]Atmospheric Environment Center, International Joint Laboratory on Climate and Environment Change (ILCEC), Nanjing University of Information Science & Technology, Nanjing 210044, China

Correspondence: Yan-Lin Zhang (dryanlinzhang@outlook.com, zhangyanlin@nuist.edu.cn)

Received: 13 February 2025 – Discussion started: 25 March 2025
Revised: 23 July 2025 – Accepted: 24 July 2025 – Published: 10 October 2025

Abstract. Hydroxymethanesulfonate (HMS) has emerged as a critical organosulfur species in ambient aerosols, yet the impact of aerosol properties, particularly ionic strength (IS), on the formation of HMS remains uncertain. Here, HMS levels in wintertime in urban Nanjing, China, were quantified at $0.30 \pm 0.10\,\mu g\,m^{-3}$, where the contribution of in-cloud formation probably carries minor significance, due to the barrier resulting from stable stratification. Elevated HMS concentrations were recorded during a Nanjing haze event, resulting from enhanced HMS formation rates, which can be largely attributed to reduced ISs on hazy days, as IS-dependent enhancement of HMS formation increased with decreasing IS within the continental IS range (6–20 $mol\,kg^{-1}$). This arises from the fact that elevated IS can boost HMS formation rate constants but also hinder the solubility of HMS precursor (SO_2) and its further dissociation. Consequently, the IS-dependent enhancement initially rose with increasing IS, peaking at $4\,mol\,kg^{-1}$, before declining. Additionally, for the first time, particulate HMS levels in marine atmospheres (Yellow Sea and Bohai Sea) were quantified, at $0.05 \pm 0.01\,\mu g\,m^{-3}$. Lower ISs (2.0–6.0 $mol\,kg^{-1}$) observed for marine aerosols exhibited more pronounced enhancements in HMS formation; this can render the aerosol-phase HMS formation a process comparable to that in cloud/fog droplets in marine environments. Furthermore, the study highlights the significant impact of ambient humidity on aerosol IS ($R = -0.89$), suggesting the integration of ionic strength in chemical models to better represent particulate sulfur chemistry, particularly in humid environments.

1 Introduction

In recent decades, hydroxymethanesulfonate (HMS) has emerged as an important organosulfur (OS) species in polluted atmospheres, particularly in northern China (Moch et al., 2018; Song et al., 2019; Ma et al., 2020; Moch et al., 2020; Wei et al., 2020; Liu et al., 2021a; Chen et al., 2022; Wang et al., 2024), where peak daily average HMS concentrations have been measured at $18.5\,\mu g\,m^{-3}$ (Ma et al., 2020). HMS is formed through aqueous-phase reactions between dissolved sulfur dioxide (SO_2) and formaldehyde (HCHO; Boyce and Hoffmann, 1984; Dixon, 1992; Zhang et al., 2023). Atmospheric chemical models have provided additional insights into the prevalence and significance of atmospheric HMS, demonstrating that HMS can account for 10 % of global aerosol sulfur in continental surface air and over 25 % in urban polluted areas during the winter season (Moch et al., 2020; Song et al., 2021; Wang et al., 2024). Regional model simulations have also suggested that, with the rising concentrations of HCHO and the heightened marine productivity of dimethyl sulfide (DMS) under climate change (Kim et al., 2018), HMS can play a progressively important role in coastal and marine aerosols (Zhao et al., 2024), potentially impacting their cloud condensation nuclei (CCN) activities (Zhang et al., 2024). However, validation of these conclusions requires observational evidence regarding the abundance of HMS in pristine coastal and even marine atmospheres.

Several measurement-based studies have suggested that meteorological conditions, specifically lower temperatures (T) and elevated relative humidity (RH), resulting in increased atmospheric liquid water content (LWC) can facilitate the dissolution of gaseous precursors, thereby accelerating aqueous-phase HMS formation (Ma et al., 2020; Wei et al., 2020; Chen et al., 2022). For instance, the HMS production rate is expected to increase linearly with the LWC (Eq. 2). In addition, other physicochemical properties of the aqueous medium (e.g., cloud/fog droplet, aerosol bulk water), including acidity (pH) and ionic strength (IS), have a more pronounced impact on HMS production (Song et al., 2019, 2021; Zhang et al., 2023). Aqueous acidity can influence HMS formation by affecting the solubility of gas-phase SO_2 and equilibrium distribution of S(IV) compounds (e.g., $SO_2{\cdot}H_2O$, HSO_3^-, and SO_3^{2-}; Berglen et al., 2004) for subsequent reaction with $HCHO_{(aq)}$. A pH range of 4 to 6 has been proposed as a favorable acidity condition for HMS formation, above which HMS can become unstable and decompose into SO_3^{2-} and $HCHO_{(aq)}$ (Boyce and Hoffmann, 1984; Olson and Hoffmann, 1986; Moch et al., 2018; Song et al., 2019). Theoretically, the HMS formation rate can decrease by a factor of 100 as pH decreases from 6 to 5, assuming a constant water content. Field observations were reported of an inverse correlation between HMS concentration and aerosol pH (Scheinhardt et al., 2014; Zhang et al., 2024). This suggests that, in realistic atmospheric environments, there are probably additional factors that play significant roles in governing HMS formation.

Recently, laboratory studies found that higher ionic strengths in aerosol water (i.e., $1 \le \mathrm{IS} \le 11\,\mathrm{mol\,kg^{-1}}$) can significantly amplify the rate constants for HMS formation (Reactions (R1) and (R2)) by 2–3 orders of magnitude, compared with dilute solution ($\mathrm{IS} < 10^{-2}\,\mathrm{mol\,kg^{-1}}$; Zhang et al., 2023). Building upon this finding, a model study revealed that the formation of HMS in aqueous aerosols can account for approximately one-third of observed HMS levels during the winter season in Beijing and also suggested that, in certain scenarios, the enhancing effect of IS can counterbalance the constraints imposed by low aerosol water content and pH values (Wang et al., 2024). Nonetheless, the exact extent and scope of this compensatory mechanism remain ambiguous. Besides, ambient aerosol properties can be highly distinct under diverse atmospheres, governed by the environmental conditions and aerosol compositions (Herrmann et al., 2015). For instance, the aerosol LWC can exhibit a wide range, from $\mu g\,m^{-3}$ in the marine atmosphere to hundreds of $\mu g\,m^{-3}$ under severe Asian haze (Gopinath et al., 2022). Aerosol particles in urban regions are commonly acidic, with pH levels spanning from 3 to 5 (Liu et al., 2021b). During haze pollution, pH values can fluctuate due to such factors as increased ammonia (NH_3) emissions or the secondary formation of sulfate, nitrate, and organic acids, potentially resulting in either an increase or a decrease in aerosol pH (Shi et al., 2019; Ruan et al., 2022). Freshly emitted sea spray aerosols can undergo rapid acidification, achieving a pH range of 3.5 to 4.7 (Yu et al., 2023), fostering conditions conducive to HMS formation. The aerosol ionic strength can also vary significantly, ranging from 1 to $20\,\mathrm{mol\,kg^{-1}}$, influenced by the aerosol composition of ionic species and the RH (Herrmann et al., 2015; Mekic and Gligorovski, 2021). For example, thermodynamic models have indicated a notably higher IS for urban aerosols ($\approx 20\,\mathrm{mol\,kg^{-1}}$; Hennigan et al., 2015), compared with marine aerosols ($\mathrm{IS} = 6.1\,\mathrm{mol\,kg^{-1}}$; Sander and Crutzen, 1996), probably attributable to the humid and pristine conditions typically found in marine atmospheres. In addition, the aforementioned properties are typically intricately interdependent within atmospheric aerosols. Thus, a comprehensive evaluation of the role of aerosol characteristics in atmospheric HMS formation, particularly the interactions between aerosol ionic strength and potentially elevated acidity across different atmospheres, is strongly desired.

In light of this, in this study, we conducted field measurements of particulate HMS levels in a continental city (Nanjing, China). As a comparison, marine aerosols were also collected during a cruise across the Yellow Sea (YS) and Bohai Sea (BS), China. The HMS abundance in collected $PM_{2.5}$ samples was quantified using ion chromatography (IC). Aerosol properties were estimated using thermodynamic models. Constrained by the precursor concentrations, the potential HMS production rates were also estimated and the role of aerosol properties in HMS formation in urban and marine environments was also examined. Results from this work shall provide improved insights on particulate sulfur chemistry within diverse atmospheric conditions.

2 Materials and methods

2.1 Atmospheric measurements in urban and marine environments

Urban aerosols and gaseous pollutants were measured in Nanjing in the winter of 2023 (Fig. S1 in the Supplement, Sect. S1). From 17 December 2023 to 10 January 2024, $PM_{2.5}$ samples were systematically collected for a duration of 23 h daily. The daily averaged concentration of HMS, together with concentrations of other water-soluble inorganic ions within $PM_{2.5}$, was determined by ion chromatography (Dionex Corp., CA, US). Given that free S(IV) or other S(IV) species, such as aldehyde-S(IV) adducts, may be misidentified as HMS in the IC analysis (Ma et al., 2020; Dingilian et al., 2024), hydrogen peroxide (H_2O_2) was employed in the analysis process to specifically isolate HMS (Dingilian et al., 2024). The results suggested that the influence of free S(IV) or other S(IV) species on HMS measurement was negligible, as elaborated in Sect. S1 in the Supplement. Carbonaceous components, including organic carbon (OC), elemental carbon (EC), and water-soluble organic carbon (WSOC), were measured using a Sunset OC/EC analyzer (Sunset Laboratory Inc.) and a total organic carbon analyzer (TOC-L, Shi-

madzu, Kyoto, Japan), respectively. The levels of gaseous pollutants (e.g., SO_2, CO, O_3) in close proximity to our sampling location were obtained from national urban air quality and real-time publishing platforms (https://quotsoft.net/air/, last access: 15 June 2025). The hourly level of formaldehyde (HCHO) was retrieved from multi-axis differential optical absorption spectroscopy (MAX-DOAS) data (Sect. S2 in the Supplement). To calculate aerosol pH, three semivolatile gases (NH_3, HNO_3, and HCl) were also monitored at 30 min intervals using a monitor for aerosols and gases (MARGA; Metrohm Ltd., Switzerland). Meteorological data (RH, temperature, wind speed, visibility, etc.) and backward trajectories (Sect. S3 in the Supplement) were also obtained. In addition, daily $PM_{2.5}$ samples, gas-phase SO_2 samples, and meteorological data were collected onboard during the open research cruise NORC2024-01 conducted in the spring of 2024 (from 13 to 25 April). Compositions of marine aerosols and ambient SO_2 levels were also characterized. Details of the sample collection and chemical analysis are described in Sect. S1 in the Supplement.

2.2 Estimation of ambient aerosol properties

Recognizing the influence of organic aerosol (OA), especially the WSOC, on aerosol properties, here we integrated two established thermodynamic models, namely the ISORROPIA II and Aerosol Inorganic–Organic Mixtures Functional Groups Activity Coefficient (AIOMFAC) models, to estimate aerosol liquid water content (ALWC), pH, and ionic strength (IS), following the methods delineated in previous work (Battaglia et al., 2019). The ISORROPIA II model (Fountoukis and Nenes, 2007) has gained widespread adoption in estimating aerosol characteristics for atmospheric particles (Nah et al., 2019; Zhang et al., 2024); it considers the thermodynamics of inorganic ions present in aerosol and their equilibrium with gas-phase HNO_3, NH_3, HCl, and H_2O, without consideration of organic constituents. Conversely, the AIOMFAC model (https://aiomfac.lab.mcgill.ca/, last access: 16 September 2024) offers the most extensive consideration of the organic–inorganic interaction but does not solve the equilibrium partitioning calculations. Thus, this study integrated both models to deliver a more comprehensive assessment of aerosol properties. In brief, inorganic PM composition (SO_4^{2-}, NO_3^-, Cl^-, NH_4^+, Ca^{2+}, K^+, and Mg^{2+}) and gaseous HNO_3, NH_3, and HCl data observed in urban Nanjing were input into ISORROPIA II under the "Forward" mode and "metastable" state to derive equilibrium concentrations of ALWC and all ionic species present under specified temperature (T) and RH conditions. Subsequently, organic components were incorporated in the inorganic matrix at the same T and RH settings, and the aerosol compositions were simulated using AIOMFAC to calculate the ALWC, pH, and IS. For marine aerosols, we adopted a particle to particle + gas partitioning fraction of NH_4^+ (ε) of 0.5, drawing from prior observations conducted in the Bohai Sea in May 2021 (Wang et al., 2022a) in light of the absence of gaseous data. Details regarding the model setup and the comparison between model outputs with inorganic-only simulations using ISORROPIA II can be found in Sect. S4 in the Supplement.

2.3 Kinetic description for HMS production

In the atmosphere, the formation of HMS requires first that its gas precursors (SO_2 and HCHO) dissolve into the water. Dissolved S(IV) (i.e., HSO_3^- and SO_3^{2-}) can subsequently react with $HCHO_{(aq)}$, leading to HMS formation:

$$HSO_3^- + HCHO_{(aq)} \overset{k_1}{\leftrightarrow} HOCH_2SO_3^-, \quad \text{(R1)}$$

$$SO_3^{2-} + HCHO_{(aq)} + H_2O \overset{k_2}{\leftrightarrow} HOCH_2SO_3^- + OH^-. \quad \text{(R2)}$$

These reactions are reversible; the first-order rate constant of HMS decomposition has been measured in previous studies, showing that the decomposition of HMS was so slow that HMS levels are predominantly controlled by formation kinetics in the typical pH range of cloud/fog and aerosol water (pH < 6) (Boyce and Hoffmann, 1984; Deister et al., 1986; Kok et al., 1986; Song et al., 2021). The variables k_1 and k_2 are the second-order rate constants of Reactions (R1) and (R2), respectively, where k_2 is ≈4 orders of magnitude larger than k_1. Thus, the HMS production can be highly sensitive to aerosol acidity, which governs the solubility and distribution of S(IV) species. The rate R_{HMS} ($M\,s^{-1}$) can be represented as

$$R_{HMS} = \left(k_1 \times [HSO_3^-] + k_2 \times [SO_3^{2-}]\right) \times [HCHO_{(aq)}]. \quad (1)$$

Furthermore, the HMS formation rate (P_{HMS}) in ambient aqueous medium (i.e., aerosol water) was calculated in units of $\mu g\,m^{-3}\,h^{-1}$:

$$P_{HMS} = R_{HMS} \times ALWC \times 3600 \times M_{HMS}, \quad (2)$$

where ALWC was estimated from thermodynamic models and M_{HMS} is the molar mass of HMS ($M_{HMS} = 111\,g\,mol^{-1}$). Here we considered the impact of aerosol ionic strength on HMS formation by determining the IS-dependent SO_2 solubility and the dissociation of H_2SO_3, as well as the rate constants (k_1 and k_2) for Reactions (R1) and (R2), as detailed in Sect. S5 in the Supplement.

3 Results and discussion

3.1 Detection of sulfur-containing species in urban and marine atmosphere

Figure 1 shows the observations for particulate sulfur-containing species (i.e., HMS and sulfate) and SO_2 levels in urban and marine atmospheres, together with $PM_{2.5}$ compositions, temperature, and relative humidity conditions. In

Figure 1. **(a–d)** Urban observations: time series of atmospheric measurements in urban Nanjing of **(a)** temperature and relative humidity; **(b)** SO_2 and HCHO levels; **(c)** HMS and sulfate concentration; **(d)** $PM_{2.5}$ composition. The gray shaded area highlighted a 7 d haze episode (27 December 2023 to 2 January 2024) with $PM_{2.5}$ mass concentration exceeding 75 $\mu g\,m^{-3}$. Other ancillary measurements in urban atmosphere, including wind speed and wind direction, $PM_{2.5}$ mass concentration, O_3, NH_3 level, fog occurrence, and cloud water content, can be found in Fig. S2 in the Supplement. **(e–h)** Marine observations: atmospheric measurements during marine cruise of **(e)** temperature and relative humidity; **(f)** SO_2; **(g)** HMS and sulfate level, where the biogenic nss-sulfate (bio-nss-sulfate) was calculated based on a previously measured bio-nss-sulfate/nss-sulfate ratio of 0.14 (Yang et al., 2015); **(h)** $PM_{2.5}$ composition.

urban Nanjing, a total of 25 daily $PM_{2.5}$ samples were collected from 17 December 2023 to 10 January 2024. The HMS concentrations ranged from 0.18 to 0.56 $\mu g\,m^{-3}$ (averaging at $0.30 \pm 0.10\,\mu g\,m^{-3}$), with corresponding sulfate concentrations varying from 2.06 to 18.03 $\mu g\,m^{-3}$ ($7.86 \pm 4.54\,\mu g\,m^{-3}$). The HMS/sulfate molar ratios fell between 2.5 % and 8.5 %, averaging at 4.6 ± 1.7 %. During the cruise, 13 marine $PM_{2.5}$ samples and SO_2 samples were synchronously collected from 13 to 25 April 2024. Due to sampler malfunction and limited sampling duration in adverse weather conditions, HMS was only detected in six daily marine aerosol samples, with lower concentrations ranging from 0.03 to 0.07 $\mu g\,m^{-3}$ ($0.05 \pm 0.01\,\mu g\,m^{-3}$). Despite the restricted sample number, this study provided the first observational evidence on HMS levels in marine atmosphere, roughly aligned with previous model-estimated HMS levels in marine atmosphere (0.03–0.09 $\mu g\,m^{-3}$; Zhao et al., 2024). The ambient concentrations of non-sea-salt sulfate (nss-SO_4^{2-}) were from 1.50 to 2.70 $\mu g\,m^{-3}$ ($2.09 \pm 0.46\,\mu g\,m^{-3}$). This notably lower particulate sulfur content in marine aerosols can probably be attributed to the lower gas-phase precursor concentration, evidenced by an average SO_2 level of 0.82 ± 0.47 ppb, compared with the SO_2 level in urban Nanjing of 2.2 ± 0.7 ppb. In addition, slightly lower HMS / sulfate molar ratios (3.0 ± 1.1 %) were observed in marine atmosphere, considering the biogenic contribution to nss-SO_4^{2-} in the spring (Zhang et al., 2013).

3.2 Elevated HMS levels during a haze pollution period in urban Nanjing

In addition, a 7 d haze pollution event (from 27 December 2023 to 2 January 2024) was observed in urban Nanjing, where notably elevated levels of HMS and sulfate were observed ($P < 0.05$). Throughout the haze event ($PM_{2.5} = 114.3 \pm 18.0\,\mu g\,m^{-3}$), the average concentrations of HMS and sulfate were 0.36 ± 0.09 and $11.4 \pm 4.0\,\mu g\,m^{-3}$, respectively, with a HMS/sulfate molar ratio of 3.5 ± 0.7 %

(Table S1 in the Supplement). It is noted that, even on hazy days, the HMS levels in our observations were significantly lower, compared with those reported in northern China during severe winter haze episodes (averaged at 4–7 $\mu g\,m^{-3}$; Ma et al., 2020; Liu et al., 2021a; Chen et al., 2022; Wang et al., 2024). Such divergence can be largely attributed to the contribution of HMS formed in cloud/fog processes, as evidenced by a previous study reporting comparable levels of HMS ($<1\,\mu g\,m^{-3}$) in Beijing to this work in the absence of cloud/fog, while peak HMS levels of 18.5 $\mu g\,m^{-3}$ were observed during fog processes (Ma et al., 2020). During our sampling period in Nanjing, there were no prolonged fog events (RH > 90 % and visibility < 1 km) lasting over 2 h (Fig. S2e). Additionally, a previous study has emphasized that although in-cloud formation processes can be much faster compared with aerosol water, given its large water content, their contribution to the near-surface aerosol composition can be negligible during China's winter haze, due to the accompanied temperature inversions and high atmospheric stability, so that the weak vertical exchange impeded the transportation of gas precursors emitted near the surface to high altitudes and the chemicals produced in the high-altitude cloud could not be easily transported to the ground (Wang et al., 2022b). Here, we utilized the vertical temperature profiles retrieved from http://weather.uwyo.edu/upperair/sounding.shtml (last access: 10 June 2025) to identify temperature inversion within the atmospheric boundary layer in the winter of Nanjing. As shown in Fig. S3 in the Supplement, a predominant occurrence of temperature inversions was noted across our observation days, characterized by inversion layers extending from the surface to altitudes of 2000 m, particularly evident on hazy days. Furthermore, days lacking temperature inversions (from 19 to 25 December 2023) were associated with negligible cloud water content (Fig. S2f), which were obtained from MERRA-2 (Modern-Era Retrospective Analysis for Research and Applications, Version 2; Gelaro et al., 2017). In line with Ma et al. (2020), we also detected HMS within $PM_{2.5}$ samples during seven non-cloud days. Therefore, given the protective effects of temperature inversion and low wind speeds (Fig. S2a), as well as reduced cloud water content prevalent during our observations, the contribution of in-cloud/fog HMS formation to observed particulate HMS levels was probably insignificant and the notably lower HMS levels further suggest that the aerosol bulk water might have served as a predominant medium for HMS formation during our observations.

Other factors, such as the levels of precursors and atmospheric oxidants, may also contribute to this divergence. For instance, during the winter haze in Beijing, the average levels of HMS and sulfate were reported to be 4 and 45 $\mu g\,m^{-3}$, respectively, with HMS/sulfate of 10 %, and the gaseous SO_2 and HCHO concentrations were recorded at 12 and 20 ppb, respectively (Ma et al., 2020). This study observed significantly lower levels of SO_2 (2.2 ± 0.7 ppb) and HCHO (5.4 ± 1.1 ppb) during the haze event. Conversely, the reduced HMS/sulfate ratio could be elucidated by the higher O_3 level in this work (43.3 ± 4.7 ppb), compared with Beijing (5 ppb), as low atmospheric oxidation levels could encourage more SO_2 to participate in the formation of HMS rather than sulfate (Song et al., 2019; Ma et al., 2020; Campbell et al., 2022).

In addition, the SO_2 concentration exhibited minimal variation throughout the entire sampling period, while the HCHO concentration (ranging from 0.88 to 7.11 ppb where data are available) increased during $PM_{2.5}$ pollution episodes (Fig. 1b). HMS levels strongly correlated with HCHO, with a Pearson correlation coefficient, R, of 0.61, but showed no correlation with SO_2 (Fig. S4 in the Supplement). However, peaks in HCHO level did not consistently coincide with peaks in HMS concentration, suggesting that other factors beyond these specific precursors, such as meteorological conditions and aerosol physicochemical properties, might exert a more significant influence on HMS formation (Campbell et al., 2022). Thus, correlation analysis between HMS levels and other factors, including PM compositions and gas pollutants, as well as meteorological conditions, were conducted, in order to delve deeper into the potential drivers behind HMS formation in the winter in Nanjing (Fig. S4). The HMS concentration exhibited strong correlations with sulfate and $PM_{2.5}$ level, with values of R of 0.87 and 0.67, respectively. The strong HMS-sulfate correlation can be partially explained by the concurrent generation of HMS and sulfate, given that both species were primarily formed through aqueous-phase S(IV) chemistry. A prior study has highlighted a strong correlation between HMS concentration and organic aerosol (OA) in Fairbanks, USA, where OA can dominate the ALWC, due to its substantial contribution to $PM_{2.5}$ mass (up to 75 %) and moderate hygroscopicity (Campbell et al., 2022). In this work, organic aerosols were also identified as crucial components in both urban and marine aerosols (Fig. S5 in the Supplement). In urban aerosols, organic aerosol mass ($OA = 1.6 \times OC$; Turpin and Lim, 2001) contributed between 10.4 % and 43.6 % to $PM_{2.5}$, where water-soluble organic carbon (WSOC) accounted for an average of 62 %. For marine aerosols, the contribution of organic OA stood at 21.4 ± 6.4 %, with nearly two-thirds constituting WSOC species. Organic components in urban aerosols, particularly WSOC, also exhibited a strong correlation with sulfate and HMS levels in our observations (Fig. S4), probably indicating their possible involvement in aqueous sulfur chemistry processes.

Here, notable correlations ($R = 0.75$) between HMS levels and RH (ranging from 37 % to 87 %) were observed, aligning with prior research, as elevated humidity can enhance the particle water uptake and subsequent gas dissolution. Additionally, HMS levels exhibited a significant correlation with temperature ($R = 0.60$), contrary to findings in Fairbanks, USA (Campbell et al., 2022), where lower temperatures were linked to enhanced solubility of SO_2 and HCHO, thereby facilitating HMS formation. It can be ex-

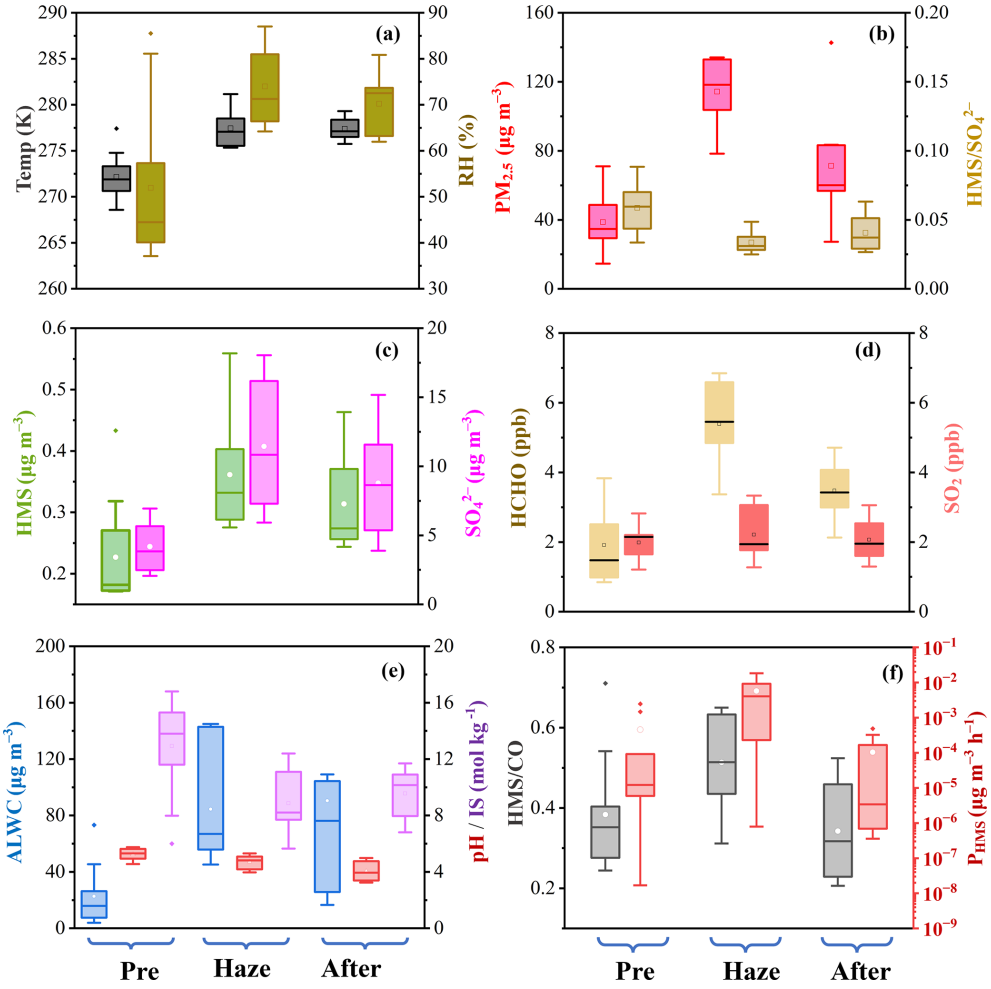

Figure 2. Averaged atmospheric characteristics under different pollution scenarios in urban Nanjing (i.e., pre-haze, haze, and after): **(a)** temperature and RH; **(b)** $PM_{2.5}$ and HMS/sulfate molar ratio; **(c)** HMS and sulfate concentration; **(d)** gas precursor levels; **(e)** aerosol properties, such as liquid water content (ALWC), pH, and ionic strength (IS); **(f)** comparison between HMS/CO ratio and HMS formation rates (P_{HMS}). Detailed values pertaining to these parameters are provided in Table S1.

plained that, in this study, higher temperatures were generally observed during haze days, typically associated with conditions favoring HMS formation, such as increased humidity and HCHO levels (Fig. 2), ultimately resulting in a positive correlation between HMS concentration and temperature. Furthermore, no significant correlation was found between HMS and wind speed (WS). The backward trajectory analysis also indicated that the air masses during haze episode predominantly originated from proximate regions (75 %), while a minor proportion (25 %) was transported from the eastern marine area (Fig. S6 in the Supplement). Collectively, these findings might suggest that observed particulate HMS levels in Nanjing are largely formed on-site in aerosol aqueous water, rather than being transported after its formation.

3.3 Role of aerosol properties in HMS formation

Therefore, the role of aerosol properties in HMS formation was further evaluated based on ALWC, pH, and ionic strength (IS) estimates from thermodynamic models (Fig. S7 in the Supplement). For urban aerosols, the estimated ALWC ranged from 4.5 to 144.9 $\mu g\,m^{-3}$ throughout the entire observation period, with elevated ALWC levels during haze pollution, averaging at $84.5 \pm 38.4\,\mu g\,m^{-3}$ (Fig. 2, Table S1). The variations in ALWC could be explained by the differences in RH and aerosol compositions, as indicated by their strong correlations. The range of aerosol pH estimates fell between 3.2 and 5.8, a range known to be favorable for HMS formation (Song et al., 2019, 2021; Moch et al., 2020). Notably, during haze pollution, the aerosol pH levels were estimated to be a half-unit lower (4.7 ± 0.5) than those on clean days (5.2 ± 0.4; Fig. 2). This trend has been reported in Nanjing (Sha et al., 2019) and other regions, such as Beijing

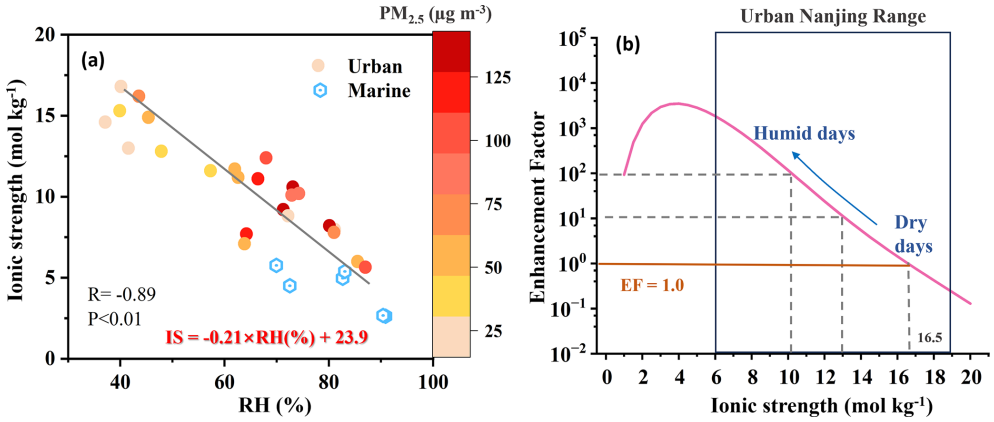

Figure 3. **(a)** Correlation between aerosol ionic strength and relative humidity level. **(b)** Enhancement factor (EF) exerted by ionic strength on HMS formation rate, calculated as $EF = P_{HMS}/P_{HMS,\,dilute}$ at a pH of 4; $P_{HMS,\,dilute}$ was calculated using the parameter proposed for dilute cloud water when the ionic strength was smaller than 1 mol kg^{-1}. Beyond this threshold (IS $\geq$ 1 mol kg^{-1}), P_{HMS} was calculated following the equations given in Table S3 in the Supplement.

(Ruan et al., 2022) and Sichuan Basin (Fu et al., 2024), a pattern frequently linked to enhanced sulfuric acid and nitric acid formation. The RH conditions and sulfate levels were identified as pivotal factors influencing pH fluctuations in this study, based on a random forest model combined with Shapley additive explanations (SHAP) analysis (Zhang et al., 2025; as detailed in Sect. S4). We also estimated the aerosol ionic strength, ranging from 5.6 to 16.8 mol kg^{-1}, falling within the typical IS range for continental aerosols (Herrmann et al., 2015). Consistent with prior research (Song et al., 2018), we noted higher ionic strengths under lower humidity conditions. A pronounced negative correlation between IS and RH ($R = -0.89$) was identified, even in situations characterized by heightened $PM_{2.5}$ levels (Fig. 3a), which can be attributed to the fact that, under high humidity conditions, an increased formation of hygroscopic species can ultimately lead to a more diluted aerosol bulk solution. Specifically, with RH increasing by 10 %, the aerosol ionic strength can decrease by around 2 units. This phenomenon accounted for the lower IS levels observed during pollution events (8.8 ± 2.1 mol kg^{-1}, 74 ± 8 %), compared with the dry and clean days before (12.9 ± 3.3 mol kg^{-1}, 52 ± 17 %). While acknowledging that the regression between RH and IS may not be universally generalizable to other regions, our findings are consistent with earlier field and model research indicating a decline in aqueous ionic concentrations on humid haze days, due to the rapid rise in ALWC (Song et al., 2018; Shen et al., 2024a; Wang et al., 2024).

HMS levels displayed a notably positive correlation with ALWC ($R = 0.67$), in agreement with prior studies (Ma et al., 2020; Campbell et al., 2022), but demonstrated an inverse relationship with pH variations and were negatively correlated with ionic strength. The inverse relation between HMS level and pH has been reported in previous studies (Scheinhardt et al., 2014; Zhang et al., 2024) but not fully explained, as it contrasted with the established HMS formation chemistry, where the HMS formation rates (P_{HMS}) can decrease, theoretically, by 10 to 100 times with 1-unit reduction in aerosol pH. Moreover, the negative correlation with ionic strength appeared to contradict earlier laboratory investigations that showed a continuous increase in reaction rate constants for Reactions (R1) and (R2) with rising IS, from <1 mol kg^{-1} (mimicking cloud/fog conditions) to 11 mol kg^{-1} (mimicking urban aerosol conditions; Zhang et al., 2023). This could be explained by dual impacts of ionic strength, which can not only enhance the reaction rate constants for Reactions (R1) and (R2) (Zhang et al., 2023) but also hinder the solubility of SO_2 and influence the dissociation constants of H_2SO_3 (Millero et al., 1989; Fig. S8 in the Supplement). Here, the IS-dependent influence on the HMS formation rate was characterized in terms of an enhancement factor (EF), calculated as $EF = P_{HMS}/P_{HMS,\,dilute}$. The value of $P_{HMS,\,dilute}$ was calculated using the classical parameters obtained in dilute solution (i.e., IS < 1 mol kg^{-1}), mimicking the condition of cloud/fog droplets (Seinfeld and Pandis, 2016). Thus, EF > 1 indicated that the ionic strength level resulted in a faster HMS formation rate compared with that within cloud/fog droplets. As shown in Fig. 3b, the IS-dependent enhancement on P_{HMS} exhibited a discontinuous response to variations in IS, showcasing peak enhancement at an IS of approximately 4 mol kg^{-1} with EF > 3000 at pH of 4, beyond which the EF gradually diminished. However, when IS surpassed 16.5 mol kg^{-1}, the EF dropped below 1.0, indicating that higher ISs may hinder, rather than promote, HMS formation. In urban Nanjing, the aerosol ionic strength (6–20 mol kg^{-1}) fell in the range where increasing IS level impeded HMS formation and every 2-unit reduction in ionic strength resulted from an 10 % increase of humidity level, which in turn accelerated the P_{HMS} by around 10 times

and also explained the observed negative correlation between HMS level and aerosol IS ($R = -0.62$).

The daily averaged steady-state P_{HMS} throughout the sampling period in Nanjing was further determined (as detailed in Sect. S5) to explore the potential role of aerosol properties, such as acidity and ionic strength, in ambient HMS formation. Given that carbon monoxide (CO) was usually considered to be an inert chemical species during rapid haze formation, with its increase often interpreted as indicative of the accumulation of primary pollutants in the shallower boundary layer (Williams et al., 2016), the ratio of HMS to CO (HMS/CO) was calculated, to better represent the secondary formation of ambient HMS (Fig. 2f). During our study period, enhanced HMS formation was noted during hazy days, as evident by the higher HMS/CO ratio (0.51 ± 0.11). The P_{HMS} estimates exhibited a good correlation with HMS/CO ($R = 0.57$; Fig. S9a) and could roughly capture the diurnal variations of HMS/CO during pollution periods. Besides, elevated HMS formation rates were found during haze events, with averaged P_{HMS} of $5.8 \pm 5.9 \times 10^{-3}\,\mu g\,m^{-3}\,h^{-1}$, an order of magnitude higher than that during the clean periods ($4.5 \pm 8.4 \times 10^{-4}\,\mu g\,m^{-3}\,h^{-1}$; Fig. 2f). Certainly, when the ionic strength effect in aerosol water was not considered, daily P_{HMS} was generally calculated to be 1 to 2 orders of magnitude lower (Fig. S9b). Notably, even with a 4-fold increase in ALWC coupled with a 2-fold increase in HCHO levels, these factors cannot completely counterbalance the potential 10-fold reduction in HMS formation rates resulting from the decreased aerosol pH, leading to slower HMS formation rates ($1.2 \pm 1.7 \times 10^{-4}\,\mu g\,m^{-3}\,h^{-1}$) during hazy days, compared with clean days ($3.3 \pm 5.3 \times 10^{-4}\,\mu g\,m^{-3}\,h^{-1}$; Fig. S9c), and failing to explain the higher HMS/CO ratios and HMS levels. Similar discrepancies have also been highlighted in previous studies where estimated HMS formation rates, without the consideration of high IS levels in aerosol water, inadequately represented the ambient HMS concentrations and their temporal fluctuations (Ma et al., 2020; Campbell et al., 2022; Zhao et al., 2024). For instance, a prior study has reported a P_{HMS} of $2.6 \times 10^{-2}\,\mu g\,m^{-3}\,h^{-1}$, which was estimated using parameters (i.e., SO_2 solubility, k_1, and k_2) obtained in dilute solution and thus failed to represent the significant HMS levels in Beijing (up to $18.5\,\mu g\,m^{-3}$; Ma et al., 2020). These results raised a possibility that the HMS formation rate could be largely underestimated without considering high ionic strengths in aerosol water. During our observation, we found that it was the reduction in aerosol ionic strength on humid and polluted days that led to more pronounced enhancement in HMS formation. This ultimately led to a nearly 10-fold rise in P_{HMS} during haze episodes, compared with dry and clean days (Fig. S9d), contributing to the elevated HMS level and HMS/CO ratio during haze events.

It was noted that the IS-dependent impacts on SO_2 solubility and H_2SO_3 dissociation constants were only measured up to $6\,mol\,kg^{-1}$ and that the effects beyond this range were extrapolated based on established relationships from experimental data (Millero et al., 1989). Building upon these extrapolations, Zhang et al. (2023) further refined the relationship between IS ($<11\,mol\,kg^{-1}$) and k_1 and k_2, based on laboratory-measured HMS formation rates, which already accounted for the potential uncertainties inherent in these extrapolation results for IS, ranging from 6 to $11\,mol\,kg^{-1}$. Consequently, it was expected that the EF calculations can effectively represent the IS effect on HMS formation rates for ISs below $11\,mol\,kg^{-1}$. However, uncertainties in EF determination at high IS levels ($>11\,mol\,kg^{-1}$) may persist, potentially contributing to the notably lower P_{HMS} predicted under high IS conditions, particularly on clean days with lower RH conditions. In addition, while aerosol HMS formation was typically thought to take place within the bulk aerosol water, the distinct characteristics of aerosol surfaces, such as a high surface-to-volume ratio or a complex and concentrated species distribution, can potentially boost the uptake of SO_2 and HCHO and thus facilitate the HMS formation process. For instance, the complex products involving HCHO with H_2O (Ervens et al., 2003) and HMS with SO_3^{2-} (Ota and Richmond, 2012), formed near or at the aerosol surface, may enhance the conversion of gas-phase precursors to aqueous phase. These processes may also contribute to the disparities between the lower HMS formation rates and ambient HMS levels. Besides, the aforementioned IS-dependent effects were determined for a well-mixed binary aqueous system containing Na^+ and Cl^- or NO_3^-, which may also introduce inaccuracies when applied to ambient aerosols. Ambient aerosols contain both water-soluble inorganic and organic compounds, together with water-insoluble organic compounds, potentially undergoing phase separation, which may lead to two distinct phases: an inorganic-rich hydrophilic phase and an organic-rich hydrophobic phase. Given that the formation of HMS necessitates the initial hydration of SO_2 succeeded by the acidic dissociation of H_2SO_3 into HSO_3^- and SO_3^{2-}, it is likely that the HMS formation predominantly proceeds within the water-rich fraction and that separated liquid phases could have differing properties (i.e., pH and ionic strength), thereby influencing the HMS formation process. Additionally, the concentrated inorganic ions in aerosol water (i.e., SO_4^{2-}, NO_3^-, Cl^-) can largely enhance the partitioning of gas-phase HCHO compared with pure water, due to the "salting-in" effect, with effective Henry's law coefficients for HCHO being 10^2–10^4 times higher than the classical value reported for pure water (Shen et al., 2024a; Zhao et al., 2024). A recent field-based study tried to formulate the effect of aqueous sulfate concentration ($C_{sulfate}$, in moles per kilogram ALWC) and the effective Henry's law coefficients for HCHO. They found that while HCHO solubility did increase with rising $C_{sulfate}$ levels, ranging from 1 to $9\,mol\,kg^{-1}$ ALWC in the winter of Beijing, hazy days experienced significantly lower HCHO solubility by 1–2 orders of magnitude, due to lower $C_{sulfate}$ values, as a result of rapid increase in ALWC. In

this study, we also observed lower $C_{sulfate}$ levels but still estimated higher P_{HMS} during haze events (Fig. S10 in the Supplement), further indicating the important role of ionic strength in promoting the formation and accumulation of HMS. Overall, the values of P_{HMS} reported here only serve as a first approximation to describe the potential daily fluctuations of HMS formation rates; further laboratory experiments conducted under more atmospherically relevant conditions (i.e., IS $> 11\,mol\,kg^{-1}$, various aerosol compositions, and aerosol-phase states) are recommended, to better refine our understanding of the impacts of ionic strength on particular sulfur chemistry.

More importantly, our results demonstrate that the discontinuous nature of IS-dependent enhancement on HMS formation allowed the reduced IS levels observed during humid and hazy days to effectively offset the inhibitory impact resulting from a half-unit decrease in aerosol pH, consequently resulting in enhanced HMS formation. This also explains the negative correlation between aerosol IS and HMS level. In a previous study, it has also been noticed that incorporating the IS effect in regional models might occasionally boost HMS formation, even under lower aerosol water content and elevated aerosol acidity conditions in urban Beijing, whereas the exact extent and scope of these compensatory mechanisms remain ambiguous.

3.4 Interplay between aerosol acidity and ionic strength in HMS formation

Sensitivity tests further revealed that a 10 % decrease in aerosol acidity and ionic strength exerted notably stronger and adverse effects on HMS production rate, compared with other factors, including ALWC, gas precursor level, and temperature (Fig. 4a). Given the commonly observed heightened humidity conditions and resultant lower ionic strength, as well as the reduction in aerosol acidity during winter haze, the interaction between aerosol acidity and ionic strength on HMS formation rates was preliminarily quantified by analyzing P_{HMS} isopleths as a function of pH and IS levels in different environmental conditions (Fig. 4b–d). Here, the averaged conditions from different environments (i.e., urban haze, urban clean, and marine atmospheres), as detailed in Table S1, were utilized in the P_{HMS} calculations. The dashed green lines, denoted EF = 1, represented the point at which P_{HMS} was equivalent to $P_{HMS,\,dilution}$, estimated for a dilute solution, mimicking conditions of cloud/fog droplets (IS $< 1\,mol\,kg^{-1}$). As depicted by the green lines, pH-dependent promotion in P_{HMS} intensified at elevated pH levels. For instance, P_{HMS} at pH 4 was approximately 30 times faster than at pH 3, and P_{HMS} at pH 6 was over 100 times faster than at pH 5. This dashed green line also exhibited a declining trend with increasing pH, suggesting that ionic strength played a more pronounced role in facilitating HMS formation within highly acidified aerosols. Furthermore, the red ridgelines at IS $\approx 4\,mol\,kg^{-1}$, which represent the IS level associated with the highest P_{HMS} at a given pH, can divide the figure into two regions. Above the ridgelines, a pH-limited regime can be identified, where HMS production rate escalated with increasing pH but diminished with rising IS levels. Conversely, below the ridgelines, a probable co-limited regime emerged, where P_{HMS} rose with both IS and pH levels, with changes amplified by variations in both factors. It is noted that there is consistent positioning of ridgelines across Fig. 4b–d, suggesting that the variations in other factors, such as precursor concentrations and ALWC, exhibit minimal impact on regulating HMS formation, compared with aerosol pH and ionic strength. In addition, we found that P_{HMS} at the ridgelines was larger than that under 1-unit higher pH at dashed green lines. These results imply that the enhancement of aerosol ionic strength level can potentially offset the inhibitory effects of more than 1-unit decrease in aqueous pH, highlighting the importance of HMS formation in aerosol water, compared with dilute solutions. In this study, urban aerosols predominantly fell within the pH-limited zone, given that their higher IS levels resulted from the prevalence of ionic species and moderate humidity conditions (Fig. 4b and d). Therefore, although aerosol pH declined during haze days (red dots in Fig. 4b), the enhancement from lower IS levels under higher humidity conditions ultimately led to higher HMS formation rates than clean days (pink dots in Fig. 4d).

Additionally, particulate sulfur chemistry, including HMS formation, has been demonstrated in coastal and marine regions (Hong et al., 2023; Zhao et al., 2024), where aerosols probably exhibited lower IS levels in comparison with continental areas, owing to the moist and pristine atmospheric conditions (Song et al., 2018). In light of this, here we also estimated the aerosol properties and the potential HMS formation rates in marine atmosphere during the cruises in YS and BS. High humidity conditions were observed, with an average value of $83\,\% \pm 6\,\%$ (Fig. 1). Chemical analysis of cruise samples revealed that the ambient concentrations of $SO_{2(g)}$, HMS, and sulfate averaged at 0.82 ± 0.47 ppb, $0.05 \pm 0.01\,\mu g\,m^{-3}$, and $2.30 \pm 0.40\,\mu g\,m^{-3}$, respectively. The estimated average characteristics of the marine aerosols included an ALWC of $14.7 \pm 6.40\,\mu g\,m^{-3}$, a pH of 4.25 ± 0.15, and an ionic strength of $4.30 \pm 1.25\,mol\,kg^{-1}$ (Table S1, Fig. S11 in the Supplement). Notably, these marine aerosols resided in the region near the ridgeline (Fig. 4c), where the ionic strength ranges exhibited more significant enhancements on HMS formation, compared with urban aerosols. In this zone, the rate of HMS formation, when factoring in the IS effect, typically surpassed that under dilute solutions, where the pH was 1 unit higher (dashed green line). This might imply the potential importance of HMS formation in ambient aerosol even amid the rapid acidification of sea salt particles due to IS-dependent enhancement. Using the averaged $[SO_{2(g)}] = 0.82$ ppb and $[HCHO_{(g)}] = 0.5$ ppb (Ervens et al., 2003; Zhao et al.,

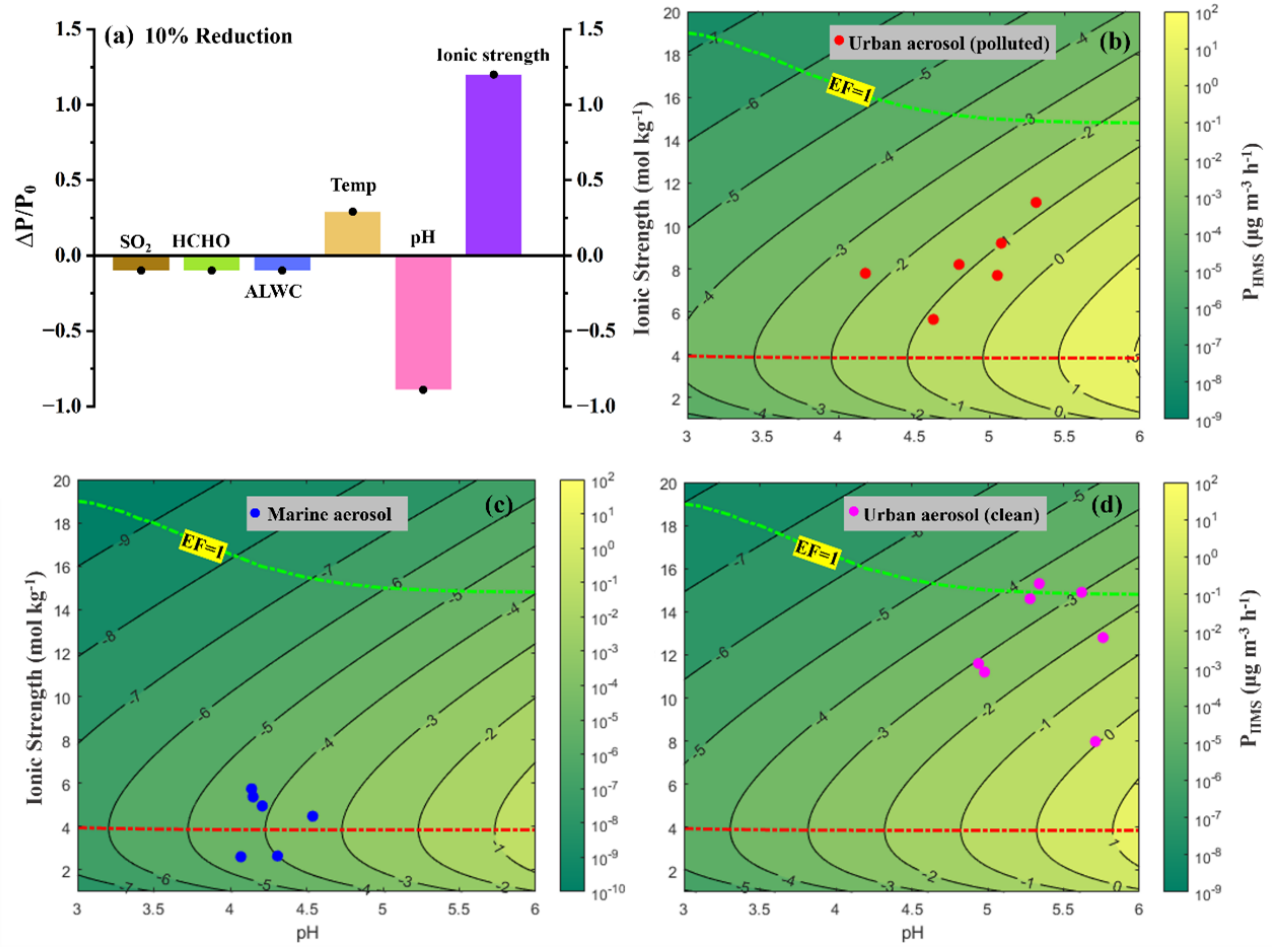

Figure 4. **(a)** Relative variation in HMS formation rate ($\Delta P/P_0$) corresponding to every 10 % reduction in SO_2 level, HCHO level, temperature, ALWC, aerosol pH, and ionic strength compared with the base scenario, where $[SO_{2(g)}] = 1$ ppb, $[HCHO_{(g)}] = 1$ ppb, $T = 278$ K, ALWC $= 100\,\mu g\,m^{-3}$, aerosol pH $= 4$, ionic strength $= 10\,mol\,kg^{-1}$. The y-axis represents the relative variation in P_{HMS}, calculated by the variation (ΔP) relative to the original value of P_{HMS} (P_0). **(b–d)** HMS formation rate (P_{HMS}) isopleths as a function of pH (ranging from 3 to 6) and ionic strength (ranging from 1 to 20 $mol\,kg^{-1}$), using the averaged atmospheric conditions from different environments, as detailed in Table S1. The aerosol droplet radius R_p was 0.15 µm (Liu et al., 2021b). Every isopleth is spaced by $10^1\,\mu g\,m^{-3}\,h^{-1}$, with the isopleth label indicating the logarithmic value of P_{HMS}. The dashed green line, denoted EF = 1, represents the point at which the value of P_{HMS}, accounting for the impact of ionic strength, equals that of P_{HMS} in a dilute scenario without considering the IS effect. The dashed red dashed represents the ridgeline associated with the IS that corresponds to the highest value of P_{HMS} at a given pH.

2024), the potential HMS formation rates in these marine aerosols were calculated to be $2.06 \times 10^{-5}\,\mu g\,m^{-3}\,h^{-1}$, a value comparable to the cloud/fog-based HMS production rate ($1.2 \times 10^{-5}\,\mu g\,m^{-3}\,h^{-1}$) reported near the Beaufort Sea (Liu et al., 2021a), with a liquid water content (LWC) of $4.8\,mg\,m^{-3}$ and a pH of 5. Considering the minimal impact of temperature inversion during our observation in April, here we also determined the in-cloud HMS formation rate to be $4.95 \times 10^{-5}\,\mu g\,m^{-3}\,h^{-1}$ in our marine environment, using a LWC of $4.8\,mg\ m^{-3}$ and a pH of 5. These results further highlight the significance of IS-dependent enhancement in HMS formation, which can render the HMS formation within aerosol water a process comparable to that observed in cloud and fog environments, particularly in humid and pristine conditions.

It is logical to see lower HMS production rates in marine aerosol compared with continental aerosols, given the lower levels of gas-phase precursors, heightened aerosol acidity, and reduced aerosol water content. These factors collectively lead to significantly diminished levels of aqueous-phase precursors, resulting in a lower formation rate. Therefore, we calculated the aqueous HMS conversion ratio by normalizing the HMS level against the stable aqueous concentration of SO_2 ($[SO_{2(aq)}]$; as shown in Eq. S7 in the Supplement), while factoring in the influences from variation in gas-phase level, aerosol water content, and acidity, to assess the role of IS on HMS formation under various atmospheric condi-

tions (Fig. S12 in the Supplement). In urban Nanjing, higher conversion ratios were observed during hazy days compared with clean days; this could probably be attributed to the impact of ionic strength, where lower IS levels exhibited more pronounced enhancement on HMS formation during haze events. Notably, despite the lower HMS and $SO_{2(g)}$ levels observed in marine aerosols, the aqueous conversion ratio for HMS was approximately twice as high as that in urban aerosols, potentially due to the HMS-formation favored ionic strength levels (ranging from 2.0 to 6.0 mol kg^{-1}) in marine aerosols.

4 Conclusion

In summary, this study provided observational evidence for ambient HMS abundance in a continental city and, for the first time, in the marine atmosphere, highlighting the ubiquity of HMS in mildly polluted and clean marine environments. Relatively lower HMS levels were observed in this work, compared with those reported in northern China. This divergence can be largely attributed to the probably minor contribution of HMS formed in cloud/fog processes. Despite this, a notable increase in HMS concentration was recorded during a 7 d haze episode in urban Nanjing. Correlation analysis highlighted that variations in HMS levels were predominantly influenced by HCHO levels, relative humidity, and aerosol properties. The significant correlation between HMS levels and higher RH has previously been associated with elevated aerosol liquid water content, which allows for more efficient dissolution of gas-phase precursors. In urban Nanjing, we also observed increased RH and HMS levels during haze events (Table S1). Moreover, ionic strength also showed a high dependence on ambient humidity ($R = -0.89$), even under high $PM_{2.5}$ scenarios, with a 10 % increase in RH level leading to a reduction of nearly 2 units in aerosol ionic strength.

Notably, even with a 4-fold increase in ALWC coupled with a 2-fold increase in HCHO levels, these factors alone cannot completely counterbalance the potential 10-fold reduction in HMS formation rates resulting from the decreased aerosol pH, and fail to explain the heightened HMS formation during pollution days. However, lower aerosol ionic strength on humid and polluted days was found to exhibit more pronounced enhancement in HMS formation, ultimately leading to a nearly 10-fold rise in P_{HMS} during haze episodes, compared with dry and clean days. This can be explained by the fact that the impact of ionic strength on HMS formation rate exhibited non-uniform responses to variations in IS levels, as the rising IS can boost the reaction rates of Reactions (R1) and (R2) while also impeding the solubility of SO_2 and affecting the dissociation constants of H_2SO_3. Specifically, the IS-dependent enhancement of HMS formation rate first increased with elevating IS levels, peaking at an IS of around 4 mol kg^{-1}, before declining. Furthermore, the dynamic interplay between aerosol ionic strength and acidity was quantified through the delineation of P_{HMS} isopleths. The results indicate that the peak enhancements exerted by IS can substantially promote HMS formation, yielding a P_{HMS} value comparable to that observed under diluted cloud/fog solution with an increase of 2 units in aqueous pH. More importantly, these results suggest that the higher relative humidity (RH) levels observed during hazy days can not only provide a greater amount of aerosol liquid water content but also dilute the urban aerosol solution toward an IS level that exhibits peak enhancement on HMS formation. Therefore, the moderate IS levels in humid environments and their enhancing effects may play a crucial role in HMS formation on urban pollution days, despite the common decrease in aerosol pH ($\Delta pH < -1$) observed during haze events (Sha et al., 2019; Ruan et al., 2022; Fu et al., 2024; Zhang et al., 2024). Additionally, lower IS levels (2.0–6.0 mol kg^{-1}), prevalent in marine aerosols, can significantly promote HMS formation within aerosol water, making this process comparable to that in cloud/fog droplets in marine atmosphere. Although the HMS formation rates were 1–2 orders of magnitude lower in marine atmosphere, compared with urban atmosphere, the aqueous conversion ratio for HMS from aqueous $SO_{2(aq)}$, when normalizing the ambient HMS level to gas-phase concentration of SO_2, aerosol liquid water content, and acidity, was nearly 2 times higher in marine aerosols than in urban aerosols; this can probably be attributed to their ionic strength, at a level conducive to HMS formation.

In addition, laboratory studies have reported that, although HMS is resistant to oxidation by H_2O_2 or O_3, it can be oxidized by $^{\bullet}OH$ through aqueous or heterogenous reactions, eventually leading to the formation of SO_4^{2-} after a series of radical chain reactions (Seinfeld and Pandis, 2016; Lai et al., 2023). Model simulations also indicate that this reaction can lead to a reduction of atmospheric concentrations of HMS by 10 %–20 % in winter and 40 %–60 % in summer, on a global scale (Song et al., 2021). More importantly, model studies underscore the potentially critical role of HMS as an atmospheric sulfur reservoir in sulfate formation (Dovrou et al., 2022; Zhao et al., 2024). This significance arises from the fact that the $HCHO_{(aq)}$ can be released during the oxidation of HMS, which can react with SO_2 to regenerate HMS and be subsequently released back into the aqueous phase during further HMS oxidation by $^{\bullet}OH$. Under such circumstances, HMS can be considered an atmospheric sulfur reservoir, with $HCHO_{(aq)}$ acting as the catalyst that facilitates the continuous conversion from gas-phase SO_2 to SO_4^{2-}. A recent modeling work indicated that this $HCHO_{(aq)}$ catalysis process could contribute up to 20 %–30 % of particulate sulfur formation under coastal and marine conditions (Zhao et al., 2024), despite the fact that uncertainties may persist due to the lack of laboratory-based kinetic parameters for HCHO-related pathways and the oversight of IS effects on HMS

and sulfate formation. Furthermore, considering the moderate ionic strength level in marine aerosol and the fact that photodecomposition of *Enteromorpha* can release substantial amounts of formaldehyde to marine atmosphere (Shen et al., 2024b), it is conceivable that HMS may play a more critical role in particulate sulfur chemistry under marine conditions. Collectively, this study provides valuable information for the prevalence of HMS and the validation of model-derived outcomes concerning HMS quantification. The work primarily concentrated on particulate HMS formation in aerosol liquid water, highlighting the role of moderate-level ionic strength in atmospheric HMS formation, and advocating for its integration in global or regional models to better represent the particulate sulfur chemistry, especially in humid environments. Nevertheless, it is noted that in-cloud HMS chemistry may also contribute to the particulate HMS levels where vertical and high-altitude observations are required to fully understand its significance, thus warranting further investigation.

Data availability. Data are available upon request from the corresponding author.

Supplement. Additional information is available on the following: collection and chemical analysis of ambient samples (Sect. S1), HCHO concentration retrieval from MAX-DOAS (Sect. S2), backward trajectory analysis (Sect. S3), aerosol property estimation (Sect. S4), steady-state HMS formation rate (P_{HMS}) calculation (Sect. S5), and aqueous HMS conversion ratio calculation (Sect. S6) in the supplement. The supplement related to this article is available online at https://doi.org/10.5194/acp-25-12721-2025-supplement.

Author contributions. RX and YLZ designed this study. RX and SB coordinated field sampling and data acquisition. FX assisted in the data visualization. RX performed the data analysis and drafted the original version of the paper. YCL and YLZ reviewed the paper and provided comments and suggestions.

Competing interests. The contact author has declared that none of the authors has any competing interests.

Disclaimer. Publisher's note: Copernicus Publications remains neutral with regard to jurisdictional claims made in the text, published maps, institutional affiliations, or any other geographical representation in this paper. While Copernicus Publications makes every effort to include appropriate place names, the final responsibility lies with the authors.

Acknowledgements. We would like to thank Cheng Liu's group at the University of Science and Technology of China for providing the hyperspectral vertical profile retrieval method and the valuable HCHO vertical profiles during our sampling period in Nanjing. These profiles support the calculation of urban HMS formation rates in our study. We also thank Zeliang Huang at Nanjing University of Information Science and Technology for assisting in the collection of marine samples.

Financial support. This work was funded by the National Natural Science Foundation of China (project number 42303083), and the Key Program of the National Natural Science Foundation of China (project number 42192512). Marine data and samples were collected onboard R/V *Lanhai101*, implementing the open research cruise NORC2024-01, supported by the NSFC Shiptime Sharing Project (project number 42349901).

Review statement. This paper was edited by Markus Ammann and reviewed by Rodney Weber and two anonymous referees.

References

Battaglia Jr., M. A., Weber, R. J., Nenes, A., and Hennigan, C. J.: Effects of water-soluble organic carbon on aerosol pH, Atmos. Chem. Phys., 19, 14607–14620, https://doi.org/10.5194/acp-19-14607-2019, 2019.

Berglen, T. F., Berntsen, T. K., Isaksen, I. S. A., and Sundet, J. K.: A global model of the coupled sulfur/oxidant chemistry in the troposphere: The sulfur cycle, J. Geophys. Res.-Atmos., 109, https://doi.org/10.1029/2003JD003948, 2004.

Boyce, S. D. and Hoffmann, M. R.: Kinetics and mechanism of the formation of hydroxymethanesulfonic acid at low pH, J. Phys. Chem., 88, 4740–4746, https://doi.org/10.1021/j150664a059, 1984.

Campbell, J. R., Battaglia Jr., M., Dingilian, K., Cesler-Maloney, M., St Clair, J. M., Hanisco, T. F., Robinson, E., DeCarlo, P., Simpson, W., Nenes, A., Weber, R. J., and Mao, J.: Source and Chemistry of Hydroxymethanesulfonate (HMS) in Fairbanks, Alaska, Environ. Sci. Technol., 56, 7657–7667, https://doi.org/10.1021/acs.est.2c00410, 2022.

Chen, C., Zhang, Z., Wei, L., Qiu, Y., Xu, W., Song, S., Sun, J., Li, Z., Chen, Y., Ma, N., Xu, W., Pan, X., Fu, P., and Sun, Y.: The importance of hydroxymethanesulfonate (HMS) in winter haze episodes in North China Plain, Environmental Research, 211, https://doi.org/10.1016/j.envres.2022.113093, 2022.

Deister, U., Neeb, R., Helas, G., and Warneck, P.: Temperature dependence of the equilibrium $CH_2(OH)_2 + HSO_3^- = CH_2(OH)SO_3^- + H_2O$ in aqueous solution, J. Phys. Chem., 90, 3213–3217, https://doi.org/10.1021/j100405a033, 1986.

Dingilian, K., Hebert, E., Battaglia, M., Jr., Campbell, J. R., Cesler-Maloney, M., Simpson, W., St. Clair, J. M., Dibb, J., Temime-Roussel, B., D'Anna, B., Moon, A., Alexander, B., Yang, Y., Nenes, A., Mao, J., and Weber, R. J.: Hydroxymethanesulfonate and Sulfur(IV) in Fairbanks Winter During the ALPACA Study, ACS ES&T Air, 1, 646–659, https://doi.org/10.1021/acsestair.4c00012, 2024.

Dixon, R. W.: Additional mass transport considerations in the formation of hydroxyalkylsulfonates, Atmos. Environ.-A, 26, 899–905, https://doi.org/10.1016/0960-1686(92)90248-J, 1992.

Dovrou, E., Bates, K. H., Moch, J. M., Mickley, L. J., Jacob, D. J., and Keutsch, F. N.: Catalytic role of formaldehyde in particulate matter formation, P. Natl. Acad. Sci. USA, 119, e2113265119, https://doi.org/10.1073/pnas.2113265119, 2022.

Ervens, B., George, C., Williams, J. E., Buxton, G. V., Salmon, G. A., Bydder, M., Wilkinson, F., Dentener, F., Mirabel, P., Wolke, R., and Herrmann, H.: CAPRAM 2.4 (MODAC mechanism): An extended and condensed tropospheric aqueous phase mechanism and its application, J. Geophys. Res.-Atmos., 108, https://doi.org/10.1029/2002JD002202, 2003.

Fountoukis, C. and Nenes, A.: ISORROPIA II: a computationally efficient thermodynamic equilibrium model for K^+–Ca^{2+}–Mg^{2+}–NH_4^+–Na^+–SO_4^{2-}–NO_3^-–Cl^-–H_2O aerosols, Atmos. Chem. Phys., 7, 4639–4659, https://doi.org/10.5194/acp-7-4639-2007, 2007.

Fu, X., Wang, X., Liu, T., He, Q., Zhang, Z., Zhang, Y., Song, W., Dai, Q., Chen, S., and Dong, F.: Secondary inorganic aerosols and aerosol acidity at different $PM_{2.5}$ pollution levels during winter haze episodes in the Sichuan Basin, China, Sci. Total Environ., 918, 170512, https://doi.org/10.1016/j.scitotenv.2024.170512, 2024.

Gelaro, R., McCarty, W., Suárez, M. J., Todling, R., Molod, A., Takacs, L., Randles, C., Darmenov, A., Bosilovich, M. G., Reichle, R., Wargan, K., Coy, L., Cullather, R., Draper, C., Akella, S., Buchard, V., Conaty, A., da Silva, A., Gu, W., Kim, G. K., Koster, R., Lucchesi, R., Merkova, D., Nielsen, J. E., Partyka, G., Pawson, S., Putman, W., Rienecker, M., Schubert, S. D., Sienkiewicz, M., and Zhao, B.: The Modern-Era Retrospective Analysis for Research and Applications, Version 2 (MERRA-2), J. Climate, 30, 5419–5454, https://doi.org/10.1175/jcli-d-16-0758.1, 2017.

Gopinath, A. K., Raj, S. S., Kommula, S. M., Jose, C., Panda, U., Bishambu, Y., Ojha, N., Ravikrishna, R., Liu, P., and Gunthe, S. S.: Complex Interplay Between Organic and Secondary Inorganic Aerosols With Ambient Relative Humidity Implicates the Aerosol Liquid Water Content Over India During Wintertime, J. Geophys. Res.-Atmos., 127, https://doi.org/10.1029/2021jd036430, 2022.

Hennigan, C. J., Izumi, J., Sullivan, A. P., Weber, R. J., and Nenes, A.: A critical evaluation of proxy methods used to estimate the acidity of atmospheric particles, Atmos. Chem. Phys., 15, 2775–2790, https://doi.org/10.5194/acp-15-2775-2015, 2015.

Herrmann, H., Schaefer, T., Tilgner, A., Styler, S. A., Weller, C., Teich, M., and Otto, T.: Tropospheric aqueous-phase chemistry: kinetics, mechanisms, and its coupling to a changing gas phase, Chemical Review, 115, 4259–4334, https://doi.org/10.1021/cr500447k, 2015.

Hong, Y., Zhang, K., Liao, D., Chen, G., Zhao, M., Lin, Y., Ji, X., Xu, K., Wu, Y., Yu, R., Hu, G., Choi, S.-D., Xue, L., and Chen, J.: Exploring the amplified role of HCHO in the formation of HMS and O_3 during the co-occurring $PM_{2.5}$ and O_3 pollution in a coastal city of southeast China, Atmos. Chem. Phys., 23, 10795–10807, https://doi.org/10.5194/acp-23-10795-2023, 2023.

Kim, A.-H., Yum, S. S., Lee, H., Chang, D. Y., and Shim, S.: Polar Cooling Effect Due to Increase of Phytoplankton and Dimethyl-Sulfide Emission, Atmosphere, 9, 384, https://doi.org/10.3390/atmos9100384, 2018.

Kok, G. L., Gitlin, S. N., and Lazrus, A. L.: Kinetics of the formation and decomposition of hydroxymethanesulfonate, J. Geophys. Res.-Atmos., 91, 2801–2804, https://doi.org/10.1029/JD091iD02p02801, 1986.

Lai, D., Wong, Y. K., Xu, R., Xing, S., Ng, S. I. M., Kong, L., Yu, J. Z., Huang, D. D., and Chan, M. N.: Significant Conversion of Organic Sulfur from Hydroxymethanesulfonate to Inorganic Sulfate and Peroxydisulfate Ions upon Heterogeneous OH Oxidation, Environ. Sci. Technol. Lett., 10, 773–778, https://doi.org/10.1021/acs.estlett.3c00472, 2023.

Liu, J., Gunsch, M. J., Moffett, C. E., Xu, L., El Asmar, R., Zhang, Q., Watson, T. B., Allen, H. M., Crounse, J. D., St. Clair, J., Kim, M., Wennberg, P. O., Weber, R. J., Sheesley, R. J., and Pratt, K. A.: Hydroxymethanesulfonate (HMS) Formation during Summertime Fog in an Arctic Oil Field, Environ. Sci. Technol. Lett., 8, 511–518, https://doi.org/10.1021/acs.estlett.1c00357, 2021a.

Liu, T., Chan, A. W. H., and Abbatt, J. P. D.: Multiphase Oxidation of Sulfur Dioxide in Aerosol Particles: Implications for Sulfate Formation in Polluted Environments, Environ. Sci. Technol., 55, 4227–4242, https://doi.org/10.1021/acs.est.0c06496, 2021b.

Ma, T., Furutani, H., Duan, F., Kimoto, T., Jiang, J., Zhang, Q., Xu, X., Wang, Y., Gao, J., Geng, G., Li, M., Song, S., Ma, Y., Che, F., Wang, J., Zhu, L., Huang, T., Toyoda, M., and He, K.: Contribution of hydroxymethanesulfonate (HMS) to severe winter haze in the North China Plain, Atmos. Chem. Phys., 20, 5887–5897, https://doi.org/10.5194/acp-20-5887-2020, 2020.

Mekic, M. and Gligorovski, S.: Ionic strength effects on heterogeneous and multiphase chemistry: Clouds versus aerosol particles, Atmos. Environ., 244, https://doi.org/10.1016/j.atmosenv.2020.117911, 2021.

Millero, F. J., Hershey, J. P., Johnson, G., and Zhang, J.-Z.: The solubility of SO_2 and the dissociation of H_2SO_3 in NaCl solutions, J. Atmos. Chem., 8, 377–389, https://doi.org/10.1007/bf00052711, 1989.

Moch, J. M., Dovrou, E., Mickley, L. J., Keutsch, F. N., Cheng, Y., Jacob, D. J., Jiang, J., Li, M., Munger, J. W., Qiao, X., and Zhang, Q.: Contribution of Hydroxymethane Sulfonate to Ambient Particulate Matter: A Potential Explanation for High Particulate Sulfur During Severe Winter Haze in Beijing, Geophys. Res. Lett., 45, https://doi.org/10.1029/2018gl079309, 2018.

Moch, J. M., Dovrou, E., Mickley, L. J., Keutsch, F. N., Liu, Z., Wang, Y., Dombek, T. L., Kuwata, M., Budisulistiorini, S. H., Yang, L., Decesari, S., Paglione, M., Alexander, B., Shao, J., Munger, J. W., and Jacob, D. J.: Global Importance of Hydroxymethanesulfonate in Ambient Particulate Matter: Implications for Air Quality, J. Geophys. Res.-Atmos., 125, e2020JD032706, https://doi.org/10.1029/2020JD032706, 2020.

Nah, T., Xu, L., Osborne-Benthaus, K. A., White, S. M., France, S., and Ng, N. L.: Mixing order of sulfate aerosols and isoprene epoxydiols affects secondary organic aerosol formation in chamber experiments, Atmos. Environ., 217, https://doi.org/10.1016/j.atmosenv.2019.116953, 2019.

Olson, T. M. and Hoffmann, M. R.: On the kinetics of formaldehyde-S(IV) adduct formation in slightly acidic solution, Atmos. Environ., 20, 2277–2278, https://doi.org/10.1016/0004-6981(86)90318-5, 1986.

Ota, S. T. and Richmond, G. L.: Uptake of SO_2 to aqueous formaldehyde surfaces, J. Am. Chem. Soc., 134, 9967–9977, https://doi.org/10.1021/ja211632r, 2012.

Ruan, X., Zhao, C., Zaveri, R. A., He, P., Wang, X., Shao, J., and Geng, L.: Simulations of aerosol pH in China using WRF-

Chem (v4.0): sensitivities of aerosol pH and its temporal variations during haze episodes, Geosci. Model Dev., 15, 6143–6164, https://doi.org/10.5194/gmd-15-6143-2022, 2022.

Sander, R. and Crutzen, P. J.: Model study indicating halogen activation and ozone destruction in polluted air masses transported to the sea, J. Geophys. Res.-Atmos., 101, 9121–9138, https://doi.org/10.1029/95jd03793, 1996.

Scheinhardt, S., van Pinxteren, D., Müller, K., Spindler, G., and Herrmann, H.: Hydroxymethanesulfonic acid in size-segregated aerosol particles at nine sites in Germany, Atmos. Chem. Phys., 14, 4531–4538, https://doi.org/10.5194/acp-14-4531-2014, 2014.

Seinfeld, J. and Pandis, S.: Atmospheric chemistry and physics: from air pollution to climate change, Wiley, ISBN 978-1-119-22117-3, 2016.

Sha, T., Ma, X., Jia, H., Tian, R., Chang, Y., Cao, F., and Zhang, Y.: Aerosol chemical component: Simulations with WRF-Chem and comparison with observations in Nanjing, Atmos. Environ., 218, 116982, https://doi.org/10.1016/j.atmosenv.2019.116982, 2019.

Shen, H., Huang, L., Qian, X., Qin, X., and Chen, Z.: Positive Feedback between Partitioning of Carbonyl Compounds and Particulate Sulfur Formation during Haze Episodes, Environ. Sci. Technol., https://doi.org/10.1021/acs.est.4c07278, 2024a.

Shen, H., Xue, L., Zhang, G., Zhu, Y., Zhao, M., Zhong, X., Nie, Y., Tang, J., Liu, Y., Yuan, Q., Gao, H., Wang, T., and Wang, W.: Marine sources of formaldehyde in the coastal atmosphere, Science Bulletin, https://doi.org/10.1016/j.scib.2024.09.024, 2024b.

Shi, G., Xu, J., Shi, X., Liu, B., Bi, X., Xiao, Z., Chen, K., Wen, J., Dong, S., Tian, Y., Feng, Y., Yu, H., Song, S., Zhao, Q., Gao, J., and Russell, A. G.: Aerosol pH Dynamics During Haze Periods in an Urban Environment in China: Use of Detailed, Hourly, Speciated Observations to Study the Role of Ammonia Availability and Secondary Aerosol Formation and Urban Environment, J. Geophys. Res.-Atmos., 124, 9730–9742, https://doi.org/10.1029/2018JD029976, 2019.

Song, S., Gao, M., Xu, W., Shao, J., Shi, G., Wang, S., Wang, Y., Sun, Y., and McElroy, M. B.: Fine-particle pH for Beijing winter haze as inferred from different thermodynamic equilibrium models, Atmos. Chem. Phys., 18, 7423–7438, https://doi.org/10.5194/acp-18-7423-2018, 2018.

Song, S., Gao, M., Xu, W., Sun, Y., Worsnop, D. R., Jayne, J. T., Zhang, Y., Zhu, L., Li, M., Zhou, Z., Cheng, C., Lv, Y., Wang, Y., Peng, W., Xu, X., Lin, N., Wang, Y., Wang, S., Munger, J. W., Jacob, D. J., and McElroy, M. B.: Possible heterogeneous chemistry of hydroxymethanesulfonate (HMS) in northern China winter haze, Atmos. Chem. Phys., 19, 1357–1371, https://doi.org/10.5194/acp-19-1357-2019, 2019.

Song, S., Ma, T., Zhang, Y., Shen, L., Liu, P., Li, K., Zhai, S., Zheng, H., Gao, M., Moch, J. M., Duan, F., He, K., and McElroy, M. B.: Global modeling of heterogeneous hydroxymethanesulfonate chemistry, Atmos. Chem. Phys., 21, 457–481, https://doi.org/10.5194/acp-21-457-2021, 2021.

Turpin, B. J. and Lim, H.-J.: Species Contributions to $PM_{2.5}$ Mass Concentrations: Revisiting Common Assumptions for Estimating Organic Mass, Aerosol Sci. Technol., 35, 602–610, https://doi.org/10.1080/02786820119445, 2001.

Wang, G., Tao, Y., Chen, J., Liu, C., Qin, X., Li, H., Yun, L., Zhang, M., Zheng, H., Gui, H., Liu, J., Huo, J., Fu, Q., Deng, C., and Huang, K.: Quantitative Decomposition of Influencing Factors to Aerosol pH Variation over the Coasts of the South China Sea, East China Sea, and Bohai Sea, Environ. Sci. Technol. Lett., 9, 815–821, https://doi.org/10.1021/acs.estlett.2c00527, 2022a.

Wang, H., Li, J., Wu, T., Ma, T., Wei, L., Zhang, H., Yang, X., Munger, J. W., Duan, F. K., Zhang, Y., Feng, Y., Zhang, Q., Sun, Y., Fu, P., McElroy, M. B., and Song, S.: Model Simulations and Predictions of Hydroxymethanesulfonate (HMS) in the Beijing-Tianjin-Hebei Region, China: Roles of Aqueous Aerosols and Atmospheric Acidity, Environ. Sci. Technol., 58, 1589–1600, https://doi.org/10.1021/acs.est.3c07306, 2024.

Wang, T., Liu, M., Liu, M., Song, Y., Xu, Z., Shang, F., Huang, X., Liao, W., Wang, W., Ge, M., Cao, J., Hu, J., Tang, G., Pan, Y., Hu, M., and Zhu, T.: Sulfate Formation Apportionment during Winter Haze Events in North China, Environ. Sci. Technol., 56, 7771–7778, https://doi.org/10.1021/acs.est.2c02533, 2022b.

Wei, L., Fu, P., Chen, X., An, N., Yue, S., Ren, H., Zhao, W., Xie, Q., Sun, Y., Zhu, Q.-F., Wang, Z., and Feng, Y.-Q.: Quantitative Determination of Hydroxymethanesulfonate (HMS) Using Ion Chromatography and UHPLC-LTQ-Orbitrap Mass Spectrometry: A Missing Source of Sulfur during Haze Episodes in Beijing, Environ. Sci. Technol. Lett., 7, 701–707, https://doi.org/10.1021/acs.estlett.0c00528, 2020.

Williams, A. G., Chambers, S. D., Conen, F., Reimann, S., Hill, M., Griffiths, A. D., and Crawford, J.: Radon as a tracer of atmospheric influences on traffic-related air pollution in a small inland city, Tellus B, 68, https://doi.org/10.3402/tellusb.v68.30967, 2016.

Yang, G.-P., Zhang, S.-H., Zhang, H.-H., Yang, J., and Liu, C.-Y.: Distribution of biogenic sulfur in the Bohai Sea and northern Yellow Sea and its contribution to atmospheric sulfate aerosol in the late fall, Marine Chemistry, 169, 23–32, https://doi.org/10.1016/j.marchem.2014.12.008, 2015.

Yu, C., Liu, T., Ge, D., Nie, W., Chi, X., and Ding, A.: Ionic Strength Enhances the Multiphase Oxidation Rate of Sulfur Dioxide by Ozone in Aqueous Aerosols: Implications for Sulfate Production in the Marine Atmosphere, Environ. Sci. Technol., 57, 6609–6615, https://doi.org/10.1021/acs.est.3c00212, 2023.

Zhang, H., Xu, Y. and Jia, L.: Hydroxymethanesulfonate formation as a significant pathway of transformation of S_2, Atmos. Environ., 294, https://doi.org/10.1016/j.atmosenv.2022.119474, 2023.

Zhang, H. H., Yang, G., Liu, C. Y., and Su, L.: Chemical Characteristics of Aerosol Composition over the Yellow Sea and the East China Sea in Autumn, J. Atmos. Sci., 70, 1784–1794, 2013.

Zhang, Y., Han, R., Sun, X., Sun, C., Griffith, S. M., Wu, G., Li, L., Li, W., Zhao, Y., Li, M., Zhou, Z., Wang, W., Sheng, L., Yu, J. Z., and Zhou, Y.: Sulfate Formation Driven by Wintertime Fog Processing and a Hydroxymethanesulfonate Complex With Iron: Observations From Single-Particle Measurements in Hong Kong, J. Geophys. Res.-Atmos., 129, https://doi.org/10.1029/2023jd040512, 2024.

Zhang, Y., Liu, Y., Ma, W., Hua, C., Zheng, F., Lian, C., Wang, W., Xia, M., Zhao, Z., Li, J., Xie, J., Wang, Z., Wang, Y., Chen, X., Zhang, Y., Feng, Z., Yan, C., Chu, B., Du, W., Kerminen, V.-M., Bianchi, F., Petäjä, T., Worsnop, D., and Kulmala, M.: Changing aerosol chemistry is redefining HONO sources, Nat. Commun., 16, https://doi.org/10.1038/s41467-025-60614-7, 2025.

Zhao, M., Shen, H., Zhang, J., Liu, Y., Sun, Y., Wang, X., Dong, C., Zhu, Y., Li, H., Shan, Y., Mu, J., Zhong, X., Tang, J., Guo, M., Wang, W., and Xue, L.: Carbonyl Compounds Regulate Atmospheric Oxidation Capacity and Particulate Sulfur Chemistry in the Coastal Atmosphere, Environ. Sci. Technol., 58, 17334–17343, https://doi.org/10.1021/acs.est.4c03947, 2024.